Individual-specific functional connectivity of the amygdala: A substrate for precision psychiatry

Chad M. Sylvester[a,1], Qiongru Yu[a], A. Benjamin Srivastava[a,b,c], Scott Marek[a], Annie Zheng[d], Dimitrios Alexopoulos[e], Christopher D. Smyser[d,e,f], Joshua S. Shimony[e], Mario Ortega[d,g], Donna L. Dierker[e], Gaurav H. Patel[b,c], Steven M. Nelson[h,i,j], Adrian W. Gilmore[k], Kathleen B. McDermott[k], Jeffrey J. Berg[l], Andrew T. Drysdale[a], Michael T. Perino[a], Abraham Z. Snyder[d,e], Ryan V. Raut[e], Timothy O. Laumann[a], Evan M. Gordon[h,i,j], Deanna M. Barch[a,e,k], Cynthia E. Rogers[a,f], Deanna J. Greene[a,e], Marcus E. Raichle[e,1], and Nico U. F. Dosenbach[d,e,f,m]

[a]Department of Psychiatry, Washington University in St. Louis, St. Louis, MO 63110; [b]Department of Psychiatry, Columbia University, New York, NY 10032; [c]New York State Psychiatric Institute, New York, NY 10032; [d]Department of Neurology, Washington University in St. Louis, St. Louis, MO 63110; [e]Department of Radiology, Washington University in St. Louis, St. Louis, MO 63110; [f]Department of Pediatrics, Washington University in St. Louis, St. Louis, MO 63110; [g]Teva Pharmaceuticals, North Wales, PA 19454; [h]VISN 17 Center of Excellence for Research on Returning War Veterans, Doris Miller VA Medical Center, Waco, TX 76711; [i]Center for Vital Longevity, University of Texas at Dallas, Dallas, TX 75235; [j]Department of Psychology and Neuroscience, Baylor University, Waco, TX 76706; [k]Department of Psychological and Brain Sciences, Washington University in St. Louis, St. Louis, MO 63110; [l]Department of Psychology, New York University, New York, NY 10003; and [m]Department of Biomedical Engineering, Washington University in St. Louis, St. Louis, MO 63110

The amygdala is central to the pathophysiology of many psychiatric illnesses. An imprecise understanding of how the amygdala fits into the larger network organization of the human brain, however, limits our ability to create models of dysfunction in individual patients to guide personalized treatment. Therefore, we investigated the position of the amygdala and its functional subdivisions within the network organization of the brain in 10 highly sampled individuals (5 h of fMRI data per person). We characterized three functional subdivisions within the amygdala of each individual. We discovered that one subdivision is preferentially correlated with the default mode network; a second is preferentially correlated with the dorsal attention and fronto-parietal networks; and third subdivision does not have any networks to which it is preferentially correlated relative to the other two subdivisions. All three subdivisions are positively correlated with ventral attention and somatomotor networks and negatively correlated with salience and cingulo-opercular networks. These observations were replicated in an independent group dataset of 120 individuals. We also found substantial across-subject variation in the distribution and magnitude of amygdala functional connectivity with the cerebral cortex that related to individual differences in the stereotactic locations both of amygdala subdivisions and of cortical functional brain networks. Finally, using lag analyses, we found consistent temporal ordering of fMRI signals in the cortex relative to amygdala subdivisions. Altogether, this work provides a detailed framework of amygdala–cortical interactions that can be used as a foundation for models relating aberrations in amygdala connectivity to psychiatric symptoms in individual patients.

amygdala | functional connectivity | fMRI

P sychiatric disorders are a leading cause of morbidity and mortality worldwide (1, 2). Over the past few decades, little progress has been made in reducing this burden, in part because we lack personalized brain-based models of mental illnesses that can be used to diagnose and guide treatment in individual patients (3). The amygdala is a structure in the medial temporal lobe that will be essential to any personalized model of mental illness that could serve to transform this outlook (4). In research settings, functional connectivity of the amygdala as measured with functional magnetic resonance imaging (fMRI) has been extensively correlated with symptoms (5–7), longitudinal course (8–10), and treatment response (11–13) in many different psychiatric disorders. A substantial roadblock in translating these research findings into clinical practice biomarkers, however, is that we have an inadequate understanding of the amygdala's role within the larger functional network organization of the brain in individuals. As a

result, we have a limited ability to create models of function and dysfunction in individual patients to guide personalized treatment.

A basic organizing principle of the human brain is that it can be divided into ∼10 to 20 large-scale, distributed functional brain networks (14–16). fMRI studies have established the connectivity properties within and between these large-scale brain networks in human adults (14, 17), as assessed by correlations in infra-slow activity (ISA, <0.1 Hz) between brain regions. Moreover, information regarding the temporal direction of these within- and between-network connections has been provided by computing the temporal offset between ISA from two brain regions that

---

Significance

Disrupted functional connectivity of the amygdala may be central to mental illness. Yet, little is known about the functional connectivity of the amygdala in individuals, limiting our ability to understand and treat amygdala dysconnectivity in individual patients. Here, we divide the amygdala into three subdivisions in each of 10 individuals and define connectivity patterns using 5 h of fMRI data per person. We demonstrate that, across individuals, each of the three amygdala subdivisions occupies a roughly consistent location and exhibits consistent functional connectivity with specific cortical functional networks: One to the default mode network, another to the dorsal attention network, and a third without preferential connectivity.

---

maximizes their correlation (18–22). Altogether, these tools have established an increasingly sophisticated network model of the human brain in which ISA propagates in specific directed patterns within and between networks. Variation in the strength and timing of these connections has been linked to risk for psychiatric illnesses (23, 24).

The biology and function of the amygdala is informed by its position within this network-level organization. Anatomical studies have delineated the cortical inputs and outputs of major amygdala nuclei in rodents (25–27) and nonhuman primates (27–30). This detailed description of the basic amygdala circuitry has led to a model in which lateral amygdala nuclei integrate sensory inputs and current physiological state, while the central amygdala nucleus sends widespread outputs to direct appropriate behavioral and physiological responses (31, 32). Pioneering work in rodents, in particular, has identified the specific cortical connections that drive amygdala responses to external stimuli (33, 34), as well as up-regulation (35, 36) and down-regulation (37, 38) of these responses. Moreover, work in both rodents (39–41) and nonhuman primates (42, 43) has linked individual variation in the behavioral response to threatening stimuli to variation in amygdala biology and cortical connectivity.

In contrast to this rich description of amygdala circuitry in rodents and nonhuman primates, we do not have a detailed description of the brain networks that connect to specific amygdala subdivisions, or of the direction and timing of these functional relations, in individual humans. Prior human fMRI studies have examined functional connections between the amygdala and specific cortical regions (44–48) and their associations with psychiatric symptoms (5–7). However, this prior work has often relied on describing functional connectivity between predefined anatomic partitions of the amygdala and cortical locations defined by averaging across large groups of subjects. Specifically, many prior studies of amygdala connectivity in humans use a single spatial template to define centromedial, superficial, and laterobasal partitions of the amygdala in all participants (44, 49–52). According to this partitioning scheme, the centromedial partition includes the central and medial nuclei; the superficial partition includes the anterior amygdaloid area, the posterior cortical nucleus, and the ventral cortical nuclei; and the laterobasal partition includes the lateral, basolateral, basomedial, and paralaminar nuclei (53, 54). This three-partition template used for imaging studies is derived from a study that examined postmortem cytoarchitecture (54) and chemoarchitecture (53) in 10 individuals at an average age of 65 y. Probabilistic locations of the centromedial, superficial, and laterobasal partitions were defined as spatial locations in which at least five of these individuals had a particular partition. Yet there was substantial variation in the location and spatial extent of the three amygdala partitions across individuals (53, 54). In addition, recent work has revealed that individuals vary in the layout of functional brain networks on the cerebral cortex (17, 55–60) and that brain–behavior relations are stronger in individualized network maps than in group-averaged templates (61). It is highly likely that this spatial variability in the location of amygdala partitions and cortical networks has confounded our ability to precisely define amygdala–cortical network relations in individuals. One consequence is that there is a suboptimal foundation for the use of amygdala functional connectivity as a biomarker in clinical settings.

In the present study, we address these challenges and place the amygdala and its subdivisions within the larger network organization of the human brain by adopting an individualized approach that is conceptually similar to the approach taken in rodents and nonhuman primates (17, 55–59). We use repeated-sampling and precision-mapping techniques to define three amygdala subdivisions separately in 10 individuals, each with 5 h of resting-state functional connectivity (rs-fc) data (the Midnight Scan Club, or "MSC" dataset) (17). Amygdala subdivisions are defined for each individual on the basis of connectivity patterns with cortex. For our primary analysis, we specifically define three data-driven amygdala subdivisions for each individual in an effort to recapitulate the tripartite models of the amygdala prevalent in the human neuroimaging literature; we also provide parallel analyses of the whole amygdala and a two-cluster solution for each individual in *SI Appendix*. Connectivity of amygdala subdivisions are related to individual-specific functional brain networks on the cortex, and lag analysis is used to determine the timing of ISA in amygdala subdivisions relative to cortical networks. The strength, direction, and timing of connectivity between the amygdala and cortex can thus be directly related to each individual brain's functional organization. For comparison, we performed the standard spatial template-defined group-based functional connectivity mapping in an independent dataset of 120 individuals collected at Washington University in St. Louis (the "WU" dataset).

Results

Individualized Amygdala Subdivisions. Standard group-based studies typically use probabilistic structural templates to divide the amygdala into three partitions, corresponding to group-average anatomical locations of the centromedial, basolateral, and superficial amygdala partitions (44, 51, 62, 63). We illustrate this publicly available template in Fig. 1*A*. Note the high degree of variability in the size and spatial extent of these partitions in the original Amunts et al. study (54). As such, these probabilistic templates may not accurately define the location of amygdala subdivisions in all individuals.

To address this issue, we developed an approach to empirically define three amygdala subdivisions separately in each of 10 individuals using functional connectivity. The number of subdivisions was set to three in order to maintain consistency with prior studies and to compare the location and variability with Amunts et al. (54). Attempts to empirically determine the "optimal" number of subdivisions within the amygdala post hoc were inconclusive, as detailed in *SI Appendix*. For completeness, we include analyses of two-cluster solutions and for the entire amygdala for each individual in *SI Appendix*. For the main analysis, three amygdala subdivisions were defined separately in each individual by clustering amygdala voxels on the basis of cortical functional connectivity patterns using *k*-means clustering. Subdivisions were matched across individuals using a similarity algorithm (see *SI Appendix* for details). Subdivisions were labeled according to the network with which they had the highest positive functional connectivity relative to the other two subdivisions, as described in greater detail below.

The empirically defined individual amygdala subdivisions (Fig. 1*B*) resemble the publicly available amygdala partitions in both average location and interindividual variability (Fig. 1*A*). One empirically defined subdivision was anatomically superior in most individuals, overlapped most strongly with the probabilistic location of the centromedial partition as quantified by the Dice coefficient (*SI Appendix*, Table S2), and is referred to as the "default mode" subdivision due to its greater connectivity with the default mode network (DMN) compared to the other amygdala subdivisions (see below). A second subdivision was located medial in most individuals, overlapped most strongly with the probabilistic location of the superficial partition, and is referred to as the "dorsal attention" subdivision due to its greater connectivity with the dorsal attention network (DAN) compared to the other amygdala subdivisions. Finally, a third subdivision was located ventral in most subjects and overlapped most strongly with the laterobasal partition. We refer to this third subdivision as the "unspecified subdivision," because it did not show preferentially stronger functional connectivity with any specific network compared to the other amygdala subdivisions; rather, it demonstrated connectivity properties that were shared across the entire amygdala. As detailed in *SI Appendix*, the alternative two-cluster solution defined subdivisions in each individual with

NEUROSCIENCE
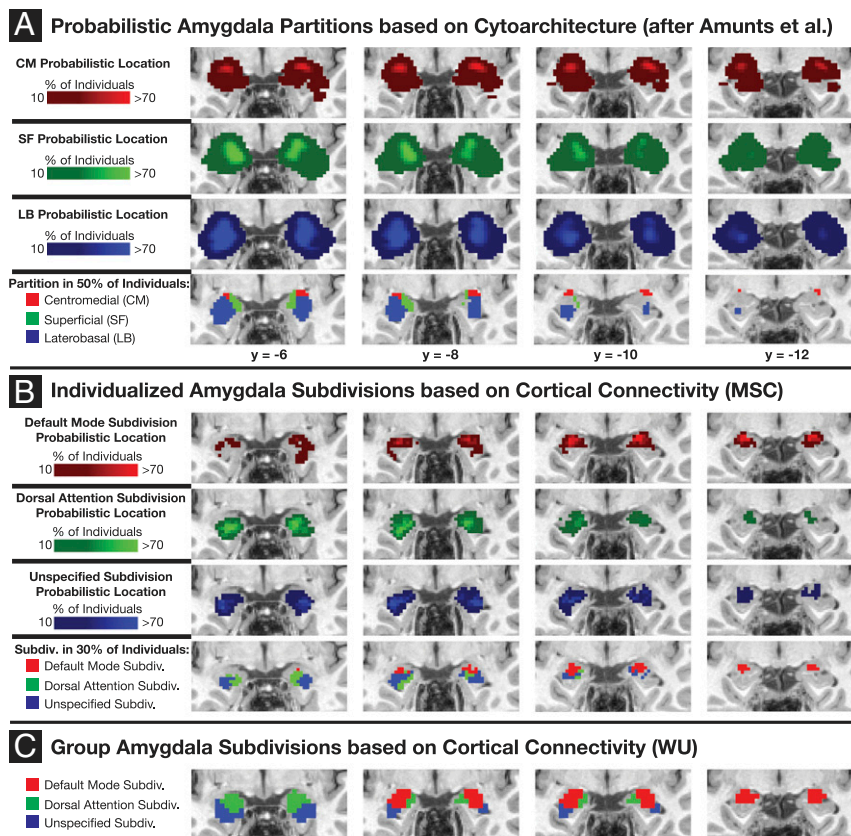
Fig. 1. Amygdala subdivisions defined in individuals on the basis of connectivity patterns to the cortex resemble amygdala partitions defined in individuals on the basis of cytoarchitecture. (*A*) Depiction of the probabilistic location of three amygdala partitions as determined postmortem by cytoarchitecture in 10 individuals from Amunts et al. (54). The spatial extent of the probabilistic partitions in this illustration are trimmed to fit within the boundaries of the amygdala as defined in the group-average WU dataset by FreeSurfer; the actual sizes of the probabilistic templates are much larger and extend into nearby white matter and cortical areas. (*B*) Depiction of data from the present study in which the locations of three amygdala subdivisions were empirically derived in 10 individuals (see text for details). Note that a default mode subdivision occupies a location similar to the centromedial partition; the dorsal attention subdivision occupies a location similar to the superficial partition; and the unspecified subdivision is spatially similar to the laterobasal partition. Note also that the variability across subjects in the location of these three subdivisions is similar to the variability present in cytoarchitecturally determined amygdala partitions. A different threshold is used to visualize the modal locations of the probabilistic partitions (50%, *Bottom* row of *A*) versus the empirically derived subdivisions (30%, *Bottom* row of *B*), because raising the threshold to 50% for the empirically derived dataset results in small areas of overlap that are difficult to visualize. The requirement for a different threshold across datasets may relate to the larger overall spatial extent of the probabilistic partitions, or could indicate that there is slightly more variability in location in the empirical subdivisions. (*C*) Empirically defined amygdala subdivisions in a group dataset of 120 individuals on the basis of cortical connectivity patterns, identical to the procedure used to define individualized subdivisions in *B*. Note the similar but not identical spatial arrangement of subdivisions compared to the other two datasets.

properties largely similar to the default mode and dorsal attention subdivisions.

Note that although the empirical, functionally defined subdivisions overlapped with the probabilistic, anatomically defined partitions on average, there was substantial across-subject variability (Fig. 1*B* and *SI Appendix,* Fig. S8). This across-subject variability appeared similar to the across-subject variability in cytoarchitectonically defined partitions in the Amunts et al. (54) study (Fig. 1*A*). A potential consequence of this variability is that applying a common template to all individuals will mislabel the amygdala subdivisions in many individuals. As a result, subdivision–cortical network relations may be obscured, a possibility that is explored in detail below.
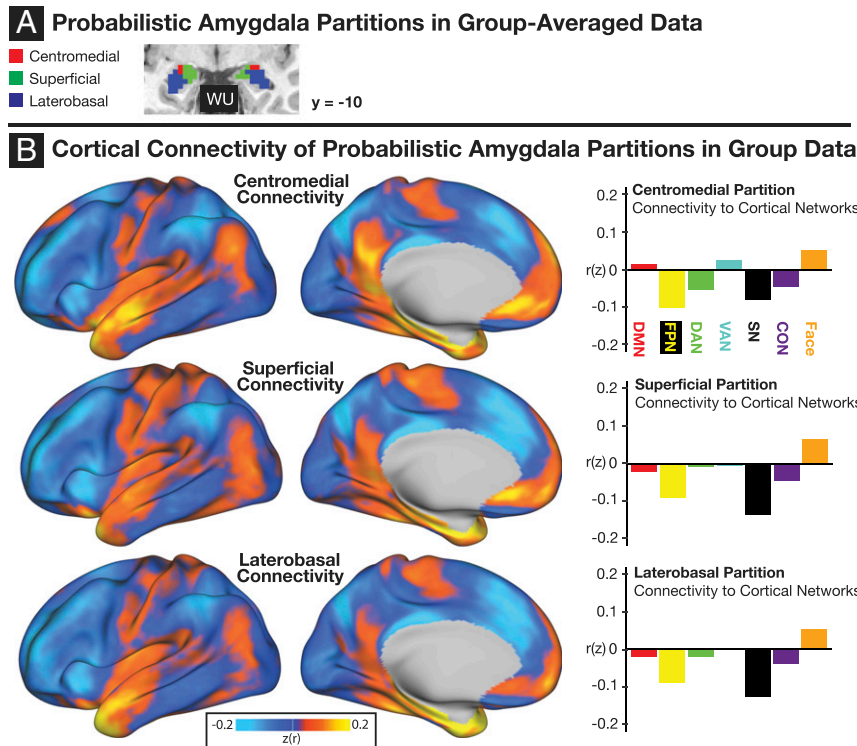
We employed the same empirical procedure to define the three subdivisions in the WU group-average dataset and obtained three similar subdivisions (Fig. 1*C*). Note that the spatial layout of these three subdivisions was similar but not identical to the probabilistic partitions in Amunts et al. (54). Dice coefficients for the overlap of each WU subdivision are listed in *SI Appendix,* Table S2.

Group-Average Functional Connectivity of Probabilistic Amygdala Partitions. We first performed the standard approach of computing cortical connectivity of each of the three probabilistic

amygdala partitions derived from Amunts et al. (54) in the group-average dataset of 120 individuals, the WU dataset. The standard template approach yielded connectivity patterns similar to prior investigations (Fig. 2) (44, 49–52). Connectivity to the cortex was highly similar across the three probabilistic amygdala partitions, as the Pearson's correlations of the whole-cortex connectivity patterns between pairs of partitions ranged from 0.88 to 0.92.

Functional Connectivity of Individualized Amygdala Subdivisions. We next computed the cortical functional connectivity of each of the three empirically and individually defined amygdala subdivisions in each of the MSC individuals (Fig. 3*A* and *SI Appendix,* Fig. S3). Each of the empirically defined subdivisions had unique patterns of connectivity to cortical networks (Fig. 3*B*). Subdivisions were named according to the network with which they had the highest positive connectivity relative to the other two subdivisions (Fig. 3*C*). A default mode subdivision had a higher magnitude of positive correlation to the DMN relative to the other two, as determined by paired t tests across the 10 MSC individuals ($P < 0.005$). A dorsal attention subdivision had higher positive connectivity to the DAN ($P < 0.001$) and fronto-parietal network (FPN, $P = 0.001$) relative to the other two subdivisions.

A Probabilistic Amygdala Partitions in Group-Averaged Data

■ Centromedial
■ Superficial
■ Laterobasal

WU   y = -10

B Cortical Connectivity of Probabilistic Amygdala Partitions in Group Data

Centromedial Connectivity

Superficial Connectivity

Laterobasal Connectivity

-0.2   0.2
z(r)

Centromedial Partition
Connectivity to Cortical Networks

DMN FPN DAN VAN SN CON Face

Superficial Partition
Connectivity to Cortical Networks

Laterobasal Partition
Connectivity to Cortical Networks

Fig. 2. The connectivity patterns of three probabilistic amygdala partitions to the cortex are highly similar to each other. (*A*) Depiction of a commonly used probabilistic template of amygdala partitions that is applied to all individuals in a group analysis. (*B*) The connectivity patterns to cortex of each of the three probabilistic partitions in a group analysis of 120 subjects. The right side of *B* computes the average connectivity of each amygdala partition to a subset of seven cortical networks (14). Connectivity to additional networks are illustrated in *SI Appendix,* Fig. S8. Face, face somatomotor network; FP, frontoparietal network.

An unspecified subdivision was not uniquely positively correlated to specific networks relative to the other subdivisions, but rather only had connectivity properties that were shared across all three subdivisions. The whole-brain connectivity pattern of the unspecified subdivision was also the least similar across individuals (average pairwise correlation = 0.29) relative to the default mode (average pairwise correlation = 0.45) and dorsal attention (average pairwise correlation = 0.35) subdivisions.

Empirical clustering of the amygdala using the group-average WU dataset also yielded default mode, dorsal attention, and unspecified subdivisions, replicating the results from the MSC dataset. To compare results from the MSC versus WU datasets, we defined "selectivity" as the difference between a cluster's connectivity to a cortical network and the average of the other two clusters' connectivity to the same network. The selectivity of the default mode and dorsal attention subdivisions for their respective networks was on average 2.2 times larger in the MSC dataset compared to the WU dataset. Similarly, within the MSC dataset, network selectivity was 2.3 times larger when using the individualized amygdala subdivisions compared to using the standard group-based template subdivisions, indicating that the individually defined subdivisions better capture network-specific functional connectivity properties of amygdala partitions in individuals. See *SI Appendix* for further details regarding these selectivity analyses.

In addition to each subdivision having unique features of connectivity with the cortex, many features of connectivity with the cortex were shared across all three subdivisions (Fig. 3*B*). For example, activity in all three subdivisions was positively correlated with activity in the ventral attention (VAN) and somatomotor (SMN) networks, and negatively correlated with activity in the cingulo-opercular (CON) and salience (SN) networks. These patterns were evident in both the individual MSC participants

(Fig. 3*B* and *SI Appendix,* Fig. S8) and the group-average WU dataset (*SI Appendix,* Fig. S5).

Amygdala Functional Connectivity Respects Functional Brain Network Boundaries. We next tested whether network specificity of amygdala subdivision functional connectivity is better captured by group-averaged functional boundaries or individual-specific functional boundaries. For this analysis, we chose to evaluate functional connectivity between the amygdala default mode subdivision and a region-of-interest (ROI) defined within the medial prefrontal cortex (mPFC), because of extensive prior work highlighting the role of amygdala–mPFC connectivity in psychiatric illnesses (64–72). Fig. 4*A* depicts functional connectivity each individual's amygdala default mode subdivision to a common, group-defined ROI centered in the mPFC at [0 33 0] in Talairach space. This ROI is derived from a metaanalysis of studies relating amygdala–mPFC connectivity to internalizing symptoms (73). Across individuals, even when using the individualized amygdala default mode subdivisions, connectivity with this group-derived mPFC region was not significantly different from zero [mean = −0.007, $t(9)$ = −0.3, P = 0.77].

We next measured individual-specific amygdala default mode subdivision functional connectivity with individual-specific functionally defined locations within the mPFC (Fig. 4*B*). In all 10 individuals, amygdala default mode subdivision connectivity was positive to the individually defined DMN portion of the mPFC [mean = 0.11, $t(9)$ = 4.7, P = 0.001] and negative to the individually defined SN portion of the mPFC [mean = −0.06, $t(8)$ = −4.0, P = 0.004]. While the location of the DMN within the mPFC had moderate overlap across individuals (average Dice coefficient: 0.61), the location of the SN was highly variable across individuals (average Dice coefficient 0.07). As depicted in
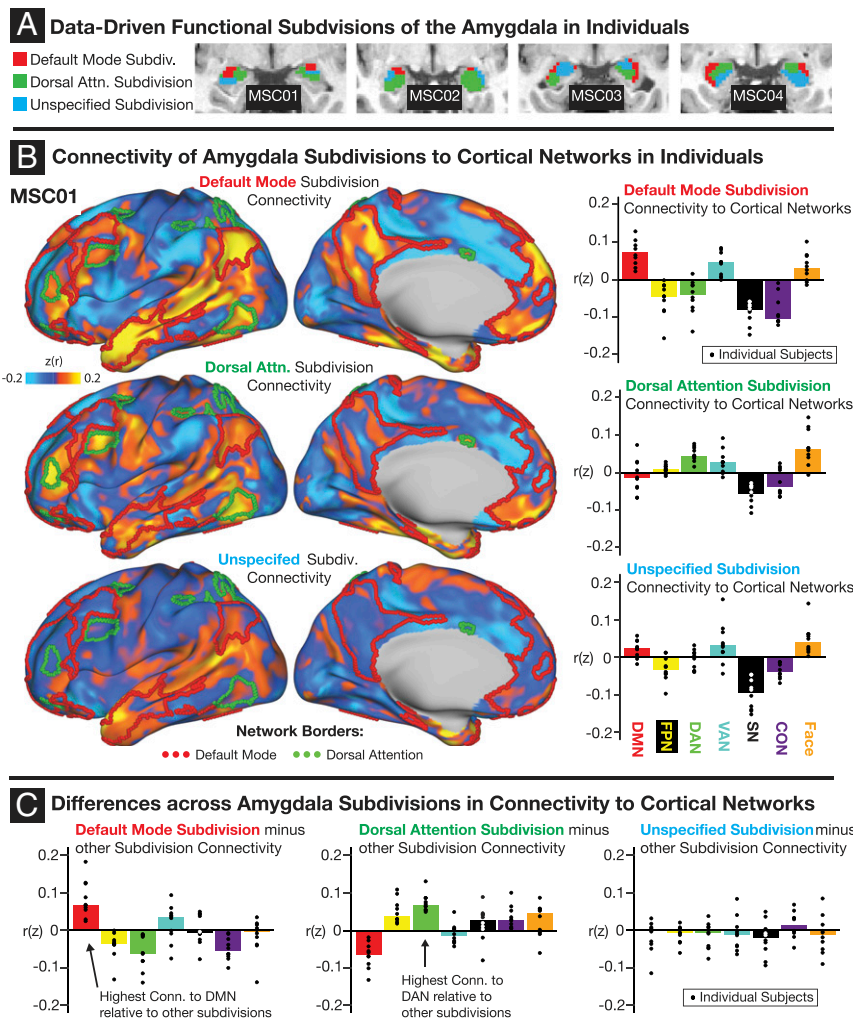
Fig. 3. Individually generated amygdala subdivisions reveal that the amygdala has one subdivision that is selectively functionally connected to the DMN and another that is selectively functionally connected to the DAN. (*A*) Depiction of the division of the amygdala into three subdivisions in four MSC individuals using *k*-means clustering (additional subjects in *SI Appendix*, Fig. S8). Voxels within the same subdivision tend to have homogenous patterns of connectivity to the cerebral cortex. The left side of *B* depicts connectivity of each amygdala subdivision to cortex in individual MSC01. Additional individuals are presented in *SI Appendix*, Fig. S3. The right side of *B* provides bar graphs that indicate the average functional connectivity of each subdivision to a subset of seven functional brain networks (additional networks in *SI Appendix*, Fig. S8). Bar height indicates the median across the 10 MSC individuals, with each individual computed separately on the basis of his or her own network map. (*C*) Provides bar graphs that depict network connectivity of each subdivision minus network connectivity of the average of the other two subdivisions. This metric is referred to as "selectivity" in the main text. Bars thus depict a measure of each subdivision's network connectivity relative to the rest of the amygdala. Individual dots represent datapoints for each individual.

Fig. 4*B*, most individuals had an island of negative connectivity (mostly corresponding to the individual-specific location of the SN) within a large swath of positive connectivity (mostly corresponding to the individual-specific location of the DMN). Because the location of the SN varies across individuals, the connectivity of the amygdala default mode subdivision to any particular stereotactic location is highly variable, and depends on the individual-specific network layout of the mPFC. These analyses suggest that, within the mPFC, connectivity with particular stereotactic locations is variable across participants because different individuals have different networks at those locations. This phenomenon is examined more broadly across the brain in the *SI Appendix*, Fig. S9.

Temporal Relationships of Amygdala Functional Connectivity to the Cortex. Lag analysis was used to explore the temporal ordering of ISA within the most robust (absolute magnitude > 0.1) cortico-amygdalar functional connections (Fig. 5*A*; see *SI Appendix* for statistical criteria). A complete list of all detected lag relations is provided in *SI Appendix*, Tables S3 and S4; here, we summarize results by subdivisions and functional brain networks. Amygdala subdivisions occupied consistent temporal positions within the larger network organization of the human brain across the MSC and WU datasets. Specifically, fMRI activity in the amygdala default mode subdivision preceded activity in the VAN and the mPFC portion of the DMN. In contrast, the amygdala default mode subdivision lagged behind other parts of the DMN such as the lateral parietal cortex (LPC). The amygdala default mode subdivision also preceded fMRI activity in the FPN but lagged behind activity in the SN, CON, and parietal memory (PMN) networks; but fMRI activity between the default mode subdivision and each of these networks was negatively correlated. The amygdala dorsal attention subdivision lagged behind the DAN, as well as the anticorrelated SN and PMN. Finally, the amygdala unspecified subdivision lagged behind the CON, SN, and PMN, all of which were anticorrelated with this subdivision. Connectivity and lag relations between each amygdala subdivision and cortical networks are depicted in Fig. 5 and *SI Appendix*, Fig. S10.

www.manaraa.com
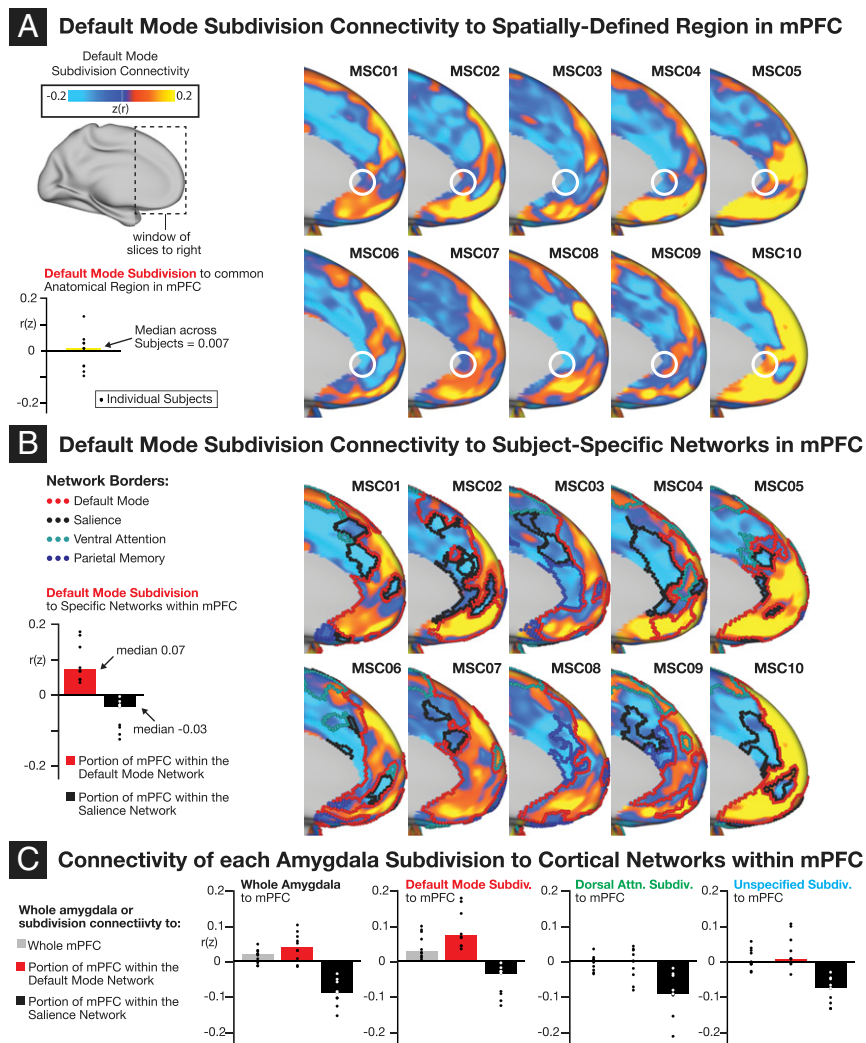
Fig. 4. Topography of amygdala functional connectivity to the cortex respects individual-specific functional network boundaries. (*A*) Placement of a common anatomical ROI over the connectivity map of the amygdala default mode subdivision in each MSC individual. This anatomical region is derived from a metaanalysis of mPFC regions in which connectivity with the amygdala is related to internalizing symptoms (73). Note the high degree of heterogeneity in the sign and magnitude of connectivity to this stereotactically defined region. The bar graph on the left depicts median connectivity across the 10 individuals, and dots indicate connectivity values for each individual. (*B*) Overlay of individual-specific network boundaries on individual amygdala functional connectivity maps for the default mode subdivision. The bar graph on the left depicts connectivity to specific networks within the mPFC; note that connectivity to these functionally defined, individual-specific regions is much more consistent than connectivity to the anatomical region in *A*. (*C*) Illustration that the positive connectivity to DMN portions of the mPFC are specific to the default mode subdivision and are not features of either the dorsal attention or somatomotor subdivisions. The bar graphs display the average amygdala functional connectivity to the mPFC (69). The gray bars display average connectivity across the entire mPFC while the red and black bars indicate average connectivity to the subset of the mPFC region that is within the DMN and SN, respectively. Separate bar graphs are presented for each subdivision within the amygdala.

Discussion

This study used an individualized approach to functional connectivity estimation to characterize the human amygdala and its subdivisions as part of the brain's global functional network organization. We found that three amygdala subdivisions each occupy roughly consistent locations across subjects and exhibit consistent functional connectivity with specific cortical functional networks. Specifically, we describe one amygdala subdivision that is located superior in most individuals and has preferential functional connectivity to the DMN; a second amygdala subdivision that is located medial in most individuals and has preferential functional connectivity to the DAN; and a third amygdala subdivision that is located ventral in most individuals and does not have any networks to which it is preferentially positively correlated. fMRI activity in all three subdivisions is positively correlated with activity in the VAN and SMN as well as

negatively correlated with activity the in CON and SN. Consistent temporal relations were detected between each amygdala subdivision and cortical functional networks in two independent datasets (WU and MSC). Notably, the stereotactic positions of both the amygdala subdivisions and the cortical functional networks varied across subjects. As a result, standard template-based approaches to measuring amygdala connectivity often capture different functional connections in different individuals. In addition to informing the basic biology of the amygdala, this work provides a framework for developing mechanistic, biologically plausible models of amygdala function and dysfunction in individual patients.

A Network-Based Framework for the Amygdala and Its Subdivisions.
We propose a network-based framework for conceptualizing amygdala functional connectivity with the cortex in humans

www.manaraa.com
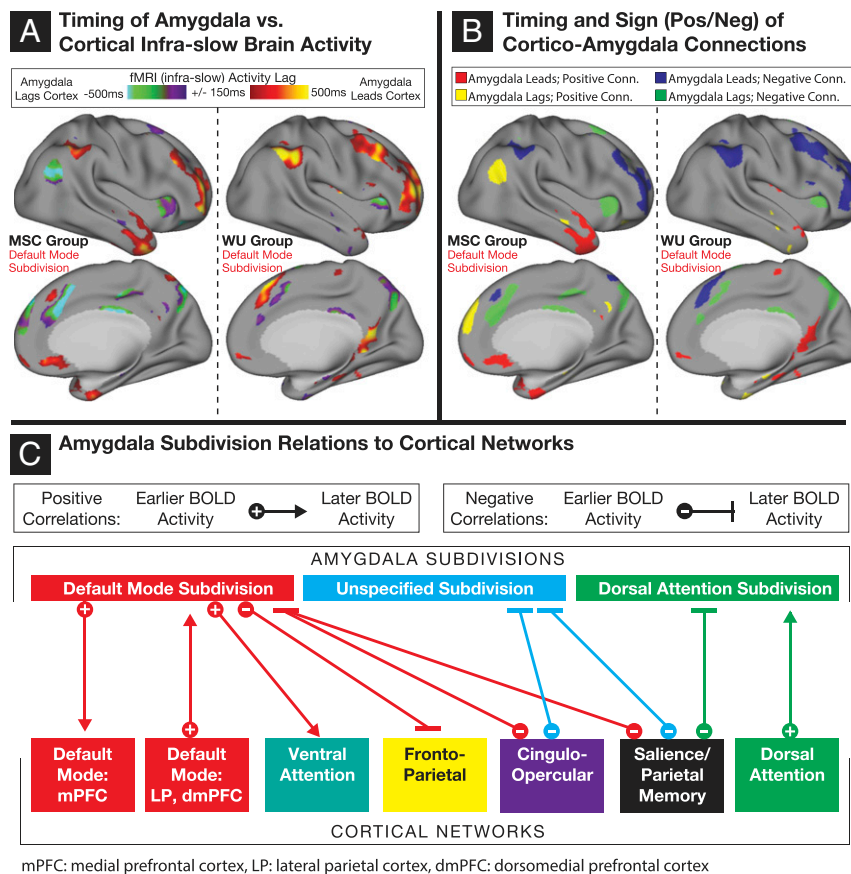
Fig. 5. Lag analysis reveals the temporal ordering of ISA in each amygdala subdivision relative to cortical networks. (*A*) Depiction of lag relations between amygdala and cortical BOLD signals in the MSC and WU group-averaged datasets. Lag relations are shown only for amygdala–cortical connections in which the magnitude of the underlying correlation is |*r*| > 0.1, because lag relations for lower correlations are less reliable. The lag relations for the default mode subdivision are depicted here; the other subdivisions are provided in *SI Appendix*, Fig. S10. Note the high degree of similarity across the two datasets. (*B*) Illustrates a conjunction map between the sign of functional connectivity (positive versus negative) and the lag direction (amygdala leads versus lags) of default mode subdivision functional connectivity to the cortex. Maps for the other two subdivisions are illustrated in *SI Appendix*, Fig. S10. (*C*) Summarizes the position of the amygdala subdivisions within the larger network organization of the human brain. This schematic displays both the sign and timing of connections between the amygdala subdivisions and cortical networks. dmPFC, dorsomedial prefrontal cortex; LP, lateral parietal cortex.

based on the observations of the magnitude and direction of connectivity between amygdala subdivisions and cortical networks outlined here. We note that fMRI time delays likely reflect ISA (<0.1 Hz) neurophysiology. Prior work suggests that ISA generally propagates in a direction opposite to higher frequency (e.g., delta) activity. According to a "sender–receiver" model, the ISA propagates from a "receiver" to a "sender" of higher frequency activity that is more likely to carry feed-forward information (18, 74). We frame the following discussion assuming this model.

Key elements of the proposed network-based framework of amygdala connectivity with the cortex are: 1) a default mode amygdala subdivision that integrates salient environmental information and past history regarding the emotional significance of these salient stimuli; 2) a dorsal attention amygdala subdivision that modulates top–down attention networks; and 3) a fundamental push–pull relation between activity in all three subdivisions of the amygdala and brain networks implicated in cognitive control. This network-based framework only becomes evident after studying individuals, because variation in the stereotactic location of amygdala subdivisions and cortical networks obscures these properties in group-average datasets.

The functional connectivity of the default mode subdivision suggests that it may integrate salient environmental information and its learned emotional significance to influence memory and

cognitive brain networks. When viewed from the vantage of the sender–receiver model, the amygdala default mode subdivision is a receiver in relation to the VAN and the mPFC portion of the DMN. The VAN is implicated in the bottom–up, involuntary orientation of spatial attention to salient stimuli, while the mPFC is implicated in extinction recall, the implicit signaling that a formerly threatening stimulus is no longer dangerous (64, 65, 75). The amygdala default mode subdivision is a sender in relation the LPC portion of the DMN, which has been linked to recall of episodic memory (76, 77). Taken together, these results are consistent with a role of the amygdala default mode subdivision in integrating information regarding the presence of salient stimuli and the past emotional significance of these stimuli in order to influence downstream memory systems.

The amygdala default mode subdivision is also a receiver in relation to the FPN and a sender in relation to the CON, SN, and PMN; however, ISA in the default mode subdivision is negatively correlated with ISA in each of these networks. These results are consistent with a relative push–pull relation between the functioning of cognitive control networks such as the FPN and CON and the functioning of emotionally based circuitry that includes the amygdala. These results further suggest that this push–pull dynamic has a specific directionality in the sender–receiver model, namely FPN → amygdala default mode subdivision → CON and SN. A speculative possibility is that these amygdala-network

www.manaraa.com

relations underlie the relative switch between emotional and cognitive processing.

The dorsal attention subdivision may influence the top–down control of spatial attention. This subdivision is a sender in relation to the DAN, which has been implicated in using goals in order to direct attention (78). Many psychiatric disorders are associated with a bias in attention toward emotional stimuli, such as a bias to attend to sad stimuli in major depression (79) and threatening stimuli in anxiety disorders (80). A speculative possibility is that the amygdala dorsal attention subdivision mediates this top–down bias in attention.

Both the dorsal attention and unspecified subdivisions are senders in relation to the SN and PMN; the unspecified subdivision is also a sender in relation to the CON. All of these subdivision–cortical interactions involve negative correlations in ISA, suggesting that they may relate to the push–pull shifts between controlled and emotionally based processing.

Relation to Animal Work. This network-based framework described above is broadly consistent with prior animal and human work. Prior anatomical tracing studies in macaques, for example, have demonstrated that only specific amygdala subnuclei are anatomically connected to regions in the mPFC and orbital frontal cortex (81), consistent with the present observation that the default mode amygdala subdivision was the only subdivision to have consistent positively correlated activity with the portion of mPFC occupied by the DMN. Prior animal studies have also reported widespread anatomical connectivity of many amygdala subnuclei with the insula, dorsal anterior cingulate, and anterior temporal lobes (27–30, 81–83). This prior animal work is consistent with functional connectivity studies of the amygdala in humans (44–46, 51, 84) and the result from the present study that the default mode, dorsal attention, and unspecified subdivisions all had significant connectivity to the SN (which includes the anterior cingulate and insular cortex) as well as to the anterior temporal lobe. A result of the present study was the detection of a dorsal attention amygdala subdivision that is functionally connected with the cortical DAN, including portions of the lateral PFC. This observation contrasts with the known anatomical connectivity to this location in nonhuman primates, which is relatively sparse or absent (29, 81). One possible explanation for this discrepancy is that correlated activity in the DAN and the amygdala dorsal attention subdivision in the human involves a multisynaptic pathway that is captured by rs-fc but not classic monosynaptic tract tracing studies. Alternatively, the dorsal attention subdivision may be a human-specific feature; additional studies are warranted to adjudicate these possibilities.

Relation to Prior Work Clustering the Human Amygdala. The spatial extent and variability of the three amygdala subdivisions defined here on the basis of functional connectivity patterns with the cortex in 10 individuals were similar to the spatial extent and variability of amygdala partitions defined on the basis of cytoarchitecture in 10 individuals by Amunts et al. (54). Specifically, the default mode subdivision paralleled the centromedial partition, the dorsal attention subdivision paralleled the superficial partition, and the unspecified subdivision is similar to the laterobasal partition. Kedo et al. (53) recently updated the work of Amunts et al. (54) by examining cytoarchitectonic borders of an expanded set of amygdala subnuclei in 15 postmortem human brains, 10 of which had been in the original Amunts et al. study. Kedo et al. (53) used novel mapping techniques to create updated probabilistic maps for use in human neuroimaging, and related these novel amygdala partitions to neurotransmitter receptor distributions of the 15 postmortem brains. The newly proposed definitions of the centromedial, superficial, and basolateral partitions of amygdala nuclei vary somewhat from the original study. Interestingly, the newly defined partitions each had a unique profile of neurotransmitter

receptor types and distribution; future work is needed to test whether the empirically defined subdivisions from the present study similarly respect receptor distributions in individuals.

Similarities between the currently defined empirical subdivisions and prior cytoarchitecture-based partitions warrant caution, however. Relating postmortem cytoarchitecture of the amygdala to MRI scans is technically challenging, and the agreement of cytoarchitecture-defined templates with subnuclei delineated on high-resolution MRI has been poor to moderate (85). Compounding this problem, there are large differences in average subject age, MRI scanner, and MRI preprocessing, including spatial registration across studies. Finally, it is well-known that functional connectivity can be present between regions without monosynaptic anatomical connectivity (86), has been shown to change in strength over the course of weeks as a result of experience (87), and is thought to reflect a prior history of simultaneous activity (15). Thus, there is no guarantee that cytoarchitecture and functional connectivity will match.

The present study is consistent with prior work that has used cortical connectivity patterns (48, 88) or coactivation patterns (89) to empirically divide the amygdala into subdivisions in group-average datasets. These prior studies have similarly detected three amygdala subdivisions in approximate spatial correspondence to the present study and Amunts et al. (54). The present study is also broadly consistent with work by Kerestes et al. (90), who examined connectivity patterns of the standard probabilistic amygdala partitions to the average locations of cortical networks in group-averaged data. The general patterns of amygdala–cortical network connectivity are similar across the two studies in terms of average magnitude of connectivity to cortical networks. In the prior group-average study, however, none of the three amygdala partitions had statistically different connectivity to a cortical network relative to the other two amygdala partitions. We suggest that these prior statistical negative results may be related to the use of group-averaged datasets that preclude precise definition of amygdala subdivisions and cortical networks in individuals.

Although the average location of the amygdala subdivisions in the present study is consistent with this prior work, there was moderate variation across the 10 subjects in the stereotactic locations of subdivisions. As a consequence, measured variation in connectivity across individuals using a group-average approach is confounded by variation in the localization of subdivisions or networks being measured. Thus, the average template is inaccurate when applied to individuals, and many subdivision-network relations will be obscured in group-average data. For example, variation in connectivity to particular stereotactic locations in the mPFC may be in part related to variation in placement of the DMN versus SN across individuals (Fig. 4).

Considerations for Defining Amygdala Subdivisions. It is important to keep in mind that results from the main analysis of the present study were obtained by forcing each subject to have exactly three amygdala subdivisions. This decision was based on substantial prior work that has divided the amygdala into three subdivisions, and our own post hoc attempts to empirically determine an "optimal" number of amygdala subdivisions were inconclusive. The overlap of the three-cluster solution in the present study with prior anatomical work by Amunts et al. (54) supports the decision to use three subdivisions. Kedo et al. (53) and other studies, however, have also described two subdivision parcellations of the amygdala, and we provide a full analysis of a two-cluster solution in *SI Appendix*. The two-cluster solution yielded subdivisions with connectivity properties similar to the default mode and dorsal attention subdivisions from the three-cluster solution. We expect that the optimal number of subdivisions within the amygdala, defined by unique patterns of connectivity to cortex, is likely to evolve as a function of data quality and scanner resolution. Furthermore, it is likely that different subdivision schemes will

provide complementary sources of information about the underlying biology of the amygdala.

Relevance of the Network-Based Framework to Neuropsychiatric Illnesses. The rich network-based framework revealed by the individual-functional approach lays the foundation for creating models of amygdala function and dysfunction in individual patients. Disrupted connectivity between the mPFC and amygdala is frequently implicated in psychiatric disorders (47, 70), as the mPFC is theorized to regulate amygdala activity implicitly via extinction memory (91). The current results are consistent with a model in which the default mode amygdala subdivision is positively correlated with, and is a receiver in relation to, portions of the mPFC that are part of the DMN, while all three amygdala subdivisions are negatively correlated with, and senders in relation to, the portion of the mPFC that is SN. The most important next step is to determine whether psychiatric disorders are associated with dysfunction (either in timing or connectivity strength) in one or all of these connections. We hypothesize that the disordered individually defined functionally based connection is likely to serve as a better biomarker than current group-derived stereotactic-based connections. The model proposed herein also suggests that intervention in these different functionally based connections would have different downstream effects on the amygdala and other cortical networks. Interventions such as deep brain stimulation or transcranial magnetic stimulation that stimulate the DMN within the mPFC might be expected to increase activity in the default mode subdivision, and perhaps cause downstream activity changes in the LPC. Stimulation of the SN within the mPFC, on the other hand, is likely to have different effects. A corollary is that stimulation of the same stereotactic location in different people is likely to affect different functional circuits and have different downstream effects; such variability may explain heterogeneity observed in stimulation-based treatments (92).

The work in the present study uses high sampling of individuals to place the amygdala and its subdivisions within the larger network organization of the human brain. We suggest that this model can serve as a framework for developing biologically plausible biomarkers and targets for intervention in individual patients with psychiatric disorders.

Methods

An overview of the methods is provided below, with details of all sections provided in *SI Appendix*.

Subjects. Two independent datasets were used for this study. The MSC subjects were 10 healthy, right-handed, young adult participants (5 females; age 24 to 34 y) recruited from the Washington University in St. Louis community and included one of the authors (N.U.F.D.) (17, 56, 57). Subject demographics are detailed in *SI Appendix*, Table S1. The replication WU dataset was an independent group-average dataset of 120 adults (60 males; average age 25 y, range 19 to 32 y). Methods for processing of this replication dataset are provided in *SI Appendix* and have been previously extensively described (93, 94). The Washington University School of Medicine Human Studies Committee and Institutional Review Board approved the study and informed consent was obtained from all participants.

MRI Image Acquisition. Imaging for the MSC individuals was performed on a Siemens TRIO 3T MRI scanner over the course of 12 separate sessions (per

subject) and included four T1-weighted images and four T2-weighted images (17). Each subject underwent 10 30-min resting-state fMRI (rs-fMRI) scans over the course of 10 separate days, for a total of 300 min of data per subject.

Resting-State Functional Connectivity Analyses. rs-fMRI preprocessing, functional connectivity processing, creation of cortical surfaces, mapping of blood oxygen-level dependent (BOLD) data to subject-specific surfaces, combination of surface and volumetric data, and generation of subject-specific functional brain network topographies have been previously described (17, 55–57) and are detailed in *SI Appendix*. Amygdala ROIs were generated by FreeSurfer 5.3 (95), hand-edited by an individual with substantial prior experience (D.A.) (95, 96), and reviewed for accuracy by a neuroradiologist (J.S.S.). Amygdala ROIs were resampled to $2 \times 2 \times 2$-mm isotropic space and ranged from 205 to 273 voxels (summed across the two hemispheres).

We computed the rs-fc of each voxel in the amygdala, for each subject. The timeseries of each amygdala voxel was correlated with each cortical vertex, regressing out cortical signal within 20 mm of the amygdala for additional artifact removal (97). We next used *k*-means clustering to empirically divide the individual amygdala voxels in each subject into three partitions on the basis of each voxel's connectivity pattern to cortex. We chose to use three clusters in an attempt to define individualized versions of the three amygdala partitions commonly explored in the prior literature on amygdala functional connectivity (44, 51, 62, 63). A similarity algorithm was used to empirically match clusters across subjects.

After deriving three clusters within the amygdala for each subject, subsequent analyses examined cluster-wise connectivity patterns. rs-fc processed BOLD timeseries were averaged across clusters for each subject and the rs-fc to cortex was recomputed, as above, for these cluster-averaged timeseries. For network-level analyses, we averaged the correlation values across cortical vertices within particular networks that were determined at the individual-subject level in a prior study (17). For the analysis of the mPFC, we used an ROI derived from a prior metaanalysis relating amygdala–mPFC connectivity to internalizing symptoms (73). The temporal ordering of signals in amygdala clusters versus cortex was determined using lag analysis as detailed in *SI Appendix* (18–20). Split-half reliability was computed for most measures to assess group- and individual-level reliability.

Data Availability. The MSC data used in this study are publicly available at OpenNeuro (https://openneuro.org/datasets/ds000224/versions/1.0.1) and NeuroVault (https://neurovault.org/collections/2447). Protocols and code are available at GitHub (https://github.com/MidnightScanClub).

1. G. B. D. Mortality; GBD 2013 Mortality and Causes of Death Collaborators, Global, regional, and national age-sex specific all-cause and cause-specific mortality for 240 causes of death, 1990-2013: A systematic analysis for the Global Burden of Disease Study 2013. *Lancet* **385**, 117–171 (2015).
2. D. Vigo, G. Thornicroft, R. Atun, Estimating the true global burden of mental illness. *Lancet Psychiatry* **3**, 171–178 (2016).
3. T. R. Insel, S. C. Landis, Twenty-five years of progress: The view from NIMH and NINDS. *Neuron* **80**, 561–567 (2013).
4. J. E. LeDoux, D. S. Pine, Using neuroscience to help understand fear and anxiety: A two-system framework. *Am. J. Psychiatry* **173**, 1083–1093 (2016).

5. T. D. Satterthwaite *et al.*, Dimensional depression severity in women with major depression and post-traumatic stress disorder correlates with fronto-amygdalar hypo-connectivty. *Mol. Psychiatry* **21**, 894–902 (2016).
6. W. Li *et al.*, Amygdala network dysfunction in late-life depression phenotypes: Relationships with symptom dimensions. *J. Psychiatr. Res.* **70**, 121–129 (2015).
7. Y. He, T. Xu, W. Zhang, X. N. Zuo, Lifespan anxiety is reflected in human amygdala cortical connectivity. *Hum. Brain Mapp.* **37**, 1178–1193 (2016).
8. C. G. Connolly *et al.*, Resting-state functional connectivity of the amygdala and longitudinal changes in depression severity in adolescent depression. *J. Affect. Disord.* **207**, 86–94 (2017).

Sylvester et al.

www.manaraa.com

9. A. M. Gard et al., Amygdala functional connectivity during socioemotional processing prospectively predicts increases in internalizing symptoms in a sample of low-income, urban, young men. *Neuroimage* **178**, 562–573 (2018).

10. Y. Zhou et al., Early altered resting-state functional connectivity predicts the severity of post-traumatic stress disorder symptoms in acutely traumatized subjects. *PLoS One* **7**, e46833 (2012).

11. K. R. Cullen et al., Neural correlates of antidepressant treatment response in adolescents with major depressive disorder. *J. Child Adolesc. Psychopharmacol.* **26**, 705–712 (2016).

12. K. K. Ellard et al., Intrinsic functional neurocircuitry associated with treatment response to transdiagnostic CBT in bipolar disorder with anxiety. *J. Affect. Disord.* **238**, 383–391 (2018).

13. M. A. Fullana et al., Basolateral amygdala-ventromedial prefrontal cortex connectivity predicts cognitive behavioural therapy outcome in adults with obsessive-compulsive disorder. *J. Psychiatry Neurosci.* **42**, 378–385 (2017).

14. J. D. Power et al., Functional network organization of the human brain. *Neuron* **72**, 665–678 (2011).

15. M. E. Raichle, The restless brain. *Brain Connect.* **1**, 3–12 (2011).

16. B. T. T. Yeo et al., The organization of the human cerebral cortex estimated by intrinsic functional connectivity. *J. Neurophysiol.* **106**, 1125–1165 (2011).

17. E. M. Gordon et al., Precision functional mapping of individual human brains. *Neuron* **95**, 791–807.e7 (2017).

18. A. Mitra et al., Spontaneous infra-slow brain activity has unique spatiotemporal dynamics and laminar structure. *Neuron* **98**, 297–305.e6 (2018).

19. A. Mitra, A. Z. Snyder, T. Blazey, M. E. Raichle, Lag threads organize the brain's intrinsic activity. *Proc. Natl. Acad. Sci. U.S.A.* **112**, E2235–E2244 (2015).

20. A. Mitra, A. Z. Snyder, C. D. Hacker, M. E. Raichle, Lag structure in resting-state fMRI. *J. Neurophysiol.* **111**, 2374–2391 (2014).

21. R. V. Raut et al., Organization of propagated intrinsic brain activity in individual humans. *Cereb. Cortex* bhz198 (2019).

22. R. V. Raut, A. Mitra, A. Z. Snyder, M. E. Raichle, On time delay estimation and sampling error in resting-state fMRI. *Neuroimage* **194**, 211–227 (2019).

23. A. Di Martino et al., Unraveling the miswired connectome: A developmental perspective. *Neuron* **83**, 1335–1353 (2014).

24. A. Mitra, A. Z. Snyder, J. N. Constantino, M. E. Raichle, The lag structure of intrinsic activity is focally altered in high functioning adults with autism. *Cereb. Cortex* **27**, 1083–1093 (2017).

25. F. Mascagni, A. J. McDonald, J. R. Coleman, Corticoamygdaloid and corticocortical projections of the rat temporal cortex: A Phaseolus vulgaris leucoagglutinin study. *Neuroscience* **57**, 697–715 (1993).

26. J. E. Krettek, J. L. Price, Projections from the amygdaloid complex to the cerebral cortex and thalamus in the rat and cat. *J. Comp. Neurol.* **172**, 687–722 (1977).

27. J. L. Price, Comparative aspects of amygdala connectivity. *Ann. N. Y. Acad. Sci.* **985**, 50–58 (2003).

28. J. P. Aggleton, M. J. Burton, R. E. Passingham, Cortical and subcortical afferents to the amygdala of the rhesus monkey (Macaca mulatta). *Brain Res.* **190**, 347–368 (1980).

29. H. T. Ghashghaei, C. C. Hilgetag, H. Barbas, Sequence of information processing for emotions based on the anatomic dialogue between prefrontal cortex and amygdala. *Neuroimage* **34**, 905–923 (2007).

30. D. Öngür, J. L. Price, The organization of networks within the orbital and medial prefrontal cortex of rats, monkeys and humans. *Cereb. Cortex* **10**, 206–219 (2000).

31. J. E. LeDoux, Emotion circuits in the brain. *Annu. Rev. Neurosci.* **23**, 155–184 (2000).

32. E. A. Phelps, J. E. LeDoux, Contributions of the amygdala to emotion processing: From animal models to human behavior. *Neuron* **48**, 175–187 (2005).

33. L. M. Romanski, J. E. LeDoux, Information cascade from primary auditory cortex to the amygdala: Corticocortical and corticoamygdaloid projections of temporal cortex in the rat. *Cereb. Cortex* **3**, 515–532 (1993).

34. L. M. Romanski, M. C. Clugnet, F. Bordi, J. E. LeDoux, Somatosensory and auditory convergence in the lateral nucleus of the amygdala. *Behav. Neurosci.* **107**, 444–450 (1993).

35. M. A. Morgan, J. E. LeDoux, Contribution of ventrolateral prefrontal cortex to the acquisition and extinction of conditioned fear in rats. *Neurobiol. Learn. Mem.* **72**, 244–251 (1999).

36. M. A. Morgan, J. E. LeDoux, Differential contribution of dorsal and ventral medial prefrontal cortex to the acquisition and extinction of conditioned fear in rats. *Behav. Neurosci.* **109**, 681–688 (1995).

37. M. A. Morgan, L. M. Romanski, J. E. LeDoux, Extinction of emotional learning: Contribution of medial prefrontal cortex. *Neurosci. Lett.* **163**, 109–113 (1993).

38. G. J. Quirk, J. S. Beer, Prefrontal involvement in the regulation of emotion: Convergence of rat and human studies. *Curr. Opin. Neurobiol.* **16**, 723–727 (2006).

39. D. E. Bush, F. Sotres-Bayon, J. E. LeDoux, Individual differences in fear: Isolating fear reactivity and fear recovery phenotypes. *J. Trauma. Stress* **20**, 413–422 (2007).

40. I. R. Galatzer-Levy, G. A. Bonanno, D. E. Bush, J. E. Ledoux, Heterogeneity in threat extinction learning: Substantive and methodological considerations for identifying individual difference in response to stress. *Front. Behav. Neurosci.* **7**, 55 (2013).

41. K. K. Cowansage, D. E. Bush, S. A. Josselyn, E. Klann, J. E. Ledoux, Basal variability in CREB phosphorylation predicts trait-like differences in amygdala-dependent memory. *Proc. Natl. Acad. Sci. U.S.A.* **110**, 16645–16650 (2013).

42. A. S. Fox et al., Functional connectivity within the primate extended amygdala is heritable and associated with early-life anxious temperament. *J. Neurosci.* **38**, 7611–7621 (2018).

43. A. J. Shackman et al., Neural mechanisms underlying heterogeneity in the presentation of anxious temperament. *Proc. Natl. Acad. Sci. U.S.A.* **110**, 6145–6150 (2013).

44. A. K. Roy et al., Functional connectivity of the human amygdala using resting state fMRI. *Neuroimage* **45**, 614–626 (2009).

45. A. X. Gorka, S. Torrisi, A. J. Shackman, C. Grillon, M. Ernst, Intrinsic functional connectivity of the central nucleus of the amygdala and bed nucleus of the stria terminalis. *Neuroimage* **168**, 392–402 (2018).

46. M. J. Kim et al., The structural and functional connectivity of the amygdala: From normal emotion to pathological anxiety. *Behav. Brain Res.* **223**, 403–410 (2011).

47. C. E. Rogers et al., Neonatal amygdala functional connectivity at rest in healthy and preterm infants and early internalizing symptoms. *J. Am. Acad. Child Adolesc. Psychiatry* **56**, 157–166 (2017).

48. K. C. Bickart, M. C. Hollenbeck, L. F. Barrett, B. C. Dickerson, Intrinsic amygdala-cortical functional connectivity predicts social network size in humans. *J. Neurosci.* **32**, 14729–14741 (2012).

49. A. K. Roy et al., Intrinsic functional connectivity of amygdala-based networks in adolescent generalized anxiety disorder. *J. Am. Acad. Child Adolesc. Psychiatry* **52**, 290–299.e2 (2013).

50. A. Etkin, K. E. Prater, A. F. Schatzberg, V. Menon, M. D. Greicius, Disrupted amygdalar subregion functional connectivity and evidence of a compensatory network in generalized anxiety disorder. *Arch. Gen. Psychiatry* **66**, 1361–1372 (2009).

51. L. J. Gabard-Durnam et al., The development of human amygdala functional connectivity at rest from 4 to 23 years: A cross-sectional study. *Neuroimage* **95**, 193–207 (2014).

52. S. Qin et al., Amygdala subregional structure and intrinsic functional connectivity predicts individual differences in anxiety during early childhood. *Biol. Psychiatry* **75**, 892–900 (2014).

53. O. Kedo et al., Receptor-driven, multimodal mapping of the human amygdala. *Brain Struct. Funct.* **223**, 1637–1666 (2018).

54. K. Amunts et al., Cytoarchitectonic mapping of the human amygdala, hippocampal region and entorhinal cortex: Intersubject variability and probability maps. *Anat. Embryol. (Berl.)* **210**, 343–352 (2005).

55. T. O. Laumann et al., Functional system and areal organization of a highly sampled individual human brain. *Neuron* **87**, 657–670 (2015).

56. T. O. Laumann et al., On the stability of BOLD fMRI correlations. *Cereb. Cortex* **27**, 4719–4732 (2017).

57. C. Gratton et al., Functional brain networks Are dominated by stable group and individual factors, not cognitive or daily variation. *Neuron* **98**, 439–452.e5 (2018).

58. D. Wang et al., Parcellating cortical functional networks in individuals. *Nat. Neurosci.* **18**, 1853–1860 (2015).

59. O. Miranda-Dominguez et al., Connectotyping: Model based fingerprinting of the functional connectome. *PLoS One* **9**, e111048 (2014).

60. S. Mueller et al., Individual variability in functional connectivity architecture of the human brain. *Neuron* **77**, 586–595 (2013).

61. R. Kong et al., Spatial topography of individual-specific cortical networks predicts human cognition, personality, and emotion. *Cereb. Cortex* **29**, 2533–2551 (2019).

62. A. K. Roy et al., Alterations in amygdala functional connectivity reflect early temperament. *Biol. Psychol.* **103**, 248–254 (2014).

63. B. C. Taber-Thomas, S. Morales, F. G. Hillary, K. E. Pérez-Edgar, Altered topography of intrinsic functional connectivity in childhood risk for social anxiety. *Depress. Anxiety* **33**, 995–1004 (2016).

64. B. J. Casey, S. S. Pattwell, C. E. Glatt, F. S. Lee, Treating the developing brain: Implications from human imaging and mouse genetics. *Annu. Rev. Med.* **64**, 427–439 (2013).

65. A. Etkin, C. Büchel, J. J. Gross, The neural bases of emotion regulation. *Nat. Rev. Neurosci.* **16**, 693–700 (2015).

66. A. Etkin, K. E. Prater, F. Hoeft, V. Menon, A. F. Schatzberg, Failure of anterior cingulate activation and connectivity with the amygdala during implicit regulation of emotional processing in generalized anxiety disorder. *Am. J. Psychiatry* **167**, 545–554 (2010).

67. A. Etkin, T. Egner, D. M. Peraza, E. R. Kandel, J. Hirsch, Resolving emotional conflict: A role for the rostral anterior cingulate cortex in modulating activity in the amygdala. *Neuron* **51**, 871–882 (2006).

68. T. A. Hare et al., Biological substrates of emotional reactivity and regulation in adolescence during an emotional go-nogo task. *Biol. Psychiatry* **63**, 927–934 (2008).

69. M. Jalbrzikowski et al., Development of white matter microstructure and intrinsic functional connectivity between the amygdala and ventromedial prefrontal cortex: Associations with anxiety and depression. *Biol. Psychiatry* **82**, 511–521 (2017).

70. M. J. Kim, D. G. Gee, R. A. Loucks, F. C. Davis, P. J. Whalen, Anxiety dissociates dorsal and ventral medial prefrontal cortex functional connectivity with the amygdala at rest. *Cereb. cortex* **21**, 1667–1673 (2011).

71. M.-F. Marin et al., Skin conductance responses and neural activations during fear conditioning and extinction recall across anxiety disorders. *JAMA Psychiatry* **74**, 622–631 (2017).

72. J. C. Motzkin, C. L. Philippi, R. C. Wolf, M. K. Baskaya, M. Koenigs, Ventromedial prefrontal cortex is critical for the regulation of amygdala activity in humans. *Biol. Psychiatry* **77**, 276–284 (2015).

73. H. A. Marusak et al., You say 'prefrontal cortex' and I say 'anterior cingulate': Meta-analysis of spatial overlap in amygdala-to-prefrontal connectivity and internalizing symptomology. *Transl. Psychiatry* **6**, e944 (2016).

74. A. Mitra et al., Human cortical-hippocampal dialogue in wake and slow-wave sleep. *Proc. Natl. Acad. Sci. U.S.A.* **113**, E6868–E6876 (2016).

75. M. R. Milad, G. J. Quirk, Fear extinction as a model for translational neuroscience: Ten years of progress. *Annu. Rev. Psychol.* **63**, 129–151 (2012).

76. A. D. Wagner, B. J. Shannon, I. Kahn, R. L. Buckner, Parietal lobe contributions to episodic memory retrieval. *Trends Cogn. Sci. (Regul. Ed.)* **9**, 445–453 (2005).

77. J. B. Hutchinson, M. R. Uncapher, A. D. Wagner, Posterior parietal cortex and episodic retrieval: Convergent and divergent effects of attention and memory. *Learn. Mem.* **16**, 343–356 (2009).

NEUROSCIENCE

Sylvester et al.

www.manaraa.com

78. M. Corbetta, G. L. Shulman, Control of goal-directed and stimulus-driven attention in the brain. *Nat. Rev. Neurosci.* **3**, 201–215 (2002).

79. A. D. Peckham, R. K. McHugh, M. W. Otto, A meta-analysis of the magnitude of biased attention in depression. *Depress. Anxiety* **27**, 1135–1142 (2010).

80. Y. Bar-Haim, D. Lamy, L. Pergamin, M. J. Bakermans-Kranenburg, M. H. van IJzendoorn, Threat-related attentional bias in anxious and nonanxious individuals: A meta-analytic study. *Psychol. Bull.* **133**, 1–24 (2007).

81. L. Stefanacci, D. G. Amaral, Some observations on cortical inputs to the macaque monkey amygdala: An anterograde tracing study. *J. Comp. Neurol.* **451**, 301–323 (2002).

82. D. S. Grayson et al., The rhesus monkey connectome predicts disrupted functional networks resulting from pharmacogenetic inactivation of the amygdala. *Neuron* **91**, 453–466 (2016).

83. J. L. Price, W. C. Drevets, Neurocircuitry of mood disorders. *Neuropsychopharmacology* **35**, 192–216 (2010).

84. D. G. Gee et al., A developmental shift from positive to negative connectivity in human amygdala-prefrontal circuitry. *J. Neurosci.* **33**, 4584–4593 (2013).

85. J. M. Tyszka, W. M. Pauli, In vivo delineation of subdivisions of the human amygdaloid complex in a high-resolution group template. *Hum. Brain Mapp.* **37**, 3979–3998 (2016).

86. J. L. Vincent et al., Intrinsic functional architecture in the anaesthetized monkey brain. *Nature* **447**, 83–86 (2007).

87. C. M. Lewis, A. Baldassarre, G. Committeri, G. L. Romani, M. Corbetta, Learning sculpts the spontaneous activity of the resting human brain. *Proc. Natl. Acad. Sci. U.S.A.* **106**, 17558–17563 (2009).

88. A. Mishra, B. P. Rogers, L. M. Chen, J. C. Gore, Functional connectivity-based parcellation of amygdala using self-organized mapping: A data driven approach. *Hum. Brain Mapp.* **35**, 1247–1260 (2014).

89. D. Bzdok, A. R. Laird, K. Zilles, P. T. Fox, S. B. Eickhoff, An investigation of the structural, connectional, and functional subspecialization in the human amygdala. *Hum. Brain Mapp.* **34**, 3247–3266 (2013).

90. R. Kerestes, H. W. Chase, M. L. Phillips, C. D. Ladouceur, S. B. Eickhoff, Multimodal evaluation of the amygdala's functional connectivity. *Neuroimage* **148**, 219–229 (2017).

91. E. A. Phelps, M. R. Delgado, K. I. Nearing, J. E. LeDoux, Extinction learning in humans: Role of the amygdala and vmPFC. *Neuron* **43**, 897–905 (2004).

92. P. E. Holtzheimer, H. S. Mayberg, Neuromodulation for treatment-resistant depression. *F1000 Med. Rep.* **4**, 22 (2012).

93. E. M. Gordon et al., Generation and evaluation of a cortical area parcellation from resting-state correlations. *Cereb. Cortex* **26**, 288–303 (2016).

94. E. M. Gordon, T. O. Laumann, B. Adeyemo, S. E. Petersen, Individual variability of the system-level organization of the human brain. *Cereb. Cortex* **27**, 386–399 (2017).

95. Z. M. Saygin et al.; Alzheimer's Disease Neuroimaging Initiative, High-resolution magnetic resonance imaging reveals nuclei of the human amygdala: Manual segmentation to automatic atlas. *Neuroimage* **155**, 370–382 (2017).

96. J. J. Entis, P. Doerga, L. F. Barrett, B. C. Dickerson, A reliable protocol for the manual segmentation of the human amygdala and its subregions using ultra-high resolution MRI. *Neuroimage* **60**, 1226–1235 (2012).

97. R. L. Buckner, F. M. Krienen, A. Castellanos, J. C. Diaz, B. T. Yeo, The organization of the human cerebellum estimated by intrinsic functional connectivity. *J. Neurophysiol.* **106**, 2322–2345 (2011).

www.manaraa.com